Solid-State Electronics 55 (2011) 54–58

Contents lists available at ScienceDirect

Solid-State Electronics

journal homepage: www.elsevier.com/locate/sse

# Spectral response of blue-sensitive Si photodetectors in SOI

J. Chu *, Z. Han, F. Meng, Z. Wang

*The Key Laboratory for Micro/Nano Technology and System of Liaoning Province, Dalian University of Technology, Liaoning Dalian 116024, China*
*Key Laboratory for Microsystem and Microfabrication of the Education Department of Liaoning Province, Liaoning Dalian 116024, China*

ARTICLE INFO

*Article history:*
Received 24 May 2010
Received in revised form 4 September 2010
Accepted 6 September 2010

The review of this paper was arranged by Prof. A. Zaslavsky

*Keywords:*
Silicon photodetector
Silicon-on-insulator
Quantum efficiency
Blue-sensitive

ABSTRACT

In this paper, we present a novel blue-sensitive Si photodetector. The detector is realized as a Si diode with a vertical PN junction in the silicon-on-insulator (SOI) thin film for normal incident light. Due to the thin SOI device layer, the photodetector shows a blue-shift spectral response with the peak external quantum efficiency (QE) of 69.6% at wavelength of 480 nm. The photodetector adopts a thin layer of $SiO_2$ as an antireflection coating and as a blocking layer for shallow ion implantation doping. The isolation trench etched through the SOI thin film to the buried oxide (BOX) provides fully electrical isolation. The device structure is simple and its performance is very high, therefore, it is in favor of monolithically integration with other micro/nanodevices.



## 1. Introduction

In recent years, SOI technology is attracting more attention from both research institutions and industry. Various top silicon layer thicknesses, ranging from a few hundred nanometers to several micrometers, are commercially available. By carefully choosing the SOI thin film, high-performance detectors with reasonable spectral response can be obtained. There have been several reports of photodiodes fabricated on SOI, especially of the prime interest for UV and fast IR applications [1–10]. However, reports of blue-sensitive SOI photodetectors are only a few cases [6–8].

The first SOI photodiode was fabricated by using laser-recrystallized technique in 1986, which was developed for optical data link and optical communication application. Its device structure was lateral p–i–n type with a dark current of 0.1 pA per 1 μm junction length under reverse bias of 5 V. Due to the thin SOI film of 440 nm, the photodetector was expected to have high speed but low spectral responsivity for long wavelength (800–850 nm) [1]. Since then, the SOI technology has made great progress. A fast SOI photodiode with an active area of 75 μm × 75 μm and a dark current of 10 pA for a reverse bias of 5 V was presented on a bonded and etched back SOI (BESOI) wafer. The thickness of the SOI film was 2.8 μm and a QE of 7.1% was achieved for a wavelength of 840 nm [2]. For other SOI photodiodes, external QE of 24% and 29% were achieved for wavelength 820 nm and 850 nm, respectively [3,4]. Few results for blue light, however, were reported. Since the open-circuit voltage ($V_{oc}$) of thin single- or polycrystalline Si solar cells increases with decreasing cell thickness, a 3-μm-thick single-crystalline Si solar cell was fabricated using a BESOI wafer. The phosphorus-doped $n^+$-layer and boron-doped $p^+$-layer were formed by thermal diffusion. The peak external QE was above 50% at around 500 nm under 0 V reverse bias voltage [5].

SOI based blue-sensitive or UV photodiodes have extensive applications, such as scintillation detector [6,7] blue-ray DVD [8] and flame detector [9]. But most of them adopted the lateral p–i–n device structure which consisted of interdigitated electrodes. Apart from the shadow effect of the metal electrodes, the surface interdigitated electrodes will also limit the detectors' integration with other micro/nanodevices at a certain extent. Another important potential application of blue-sensitive photodiodes may lie in the detection of skylight polarization pattern and polarization vision. Research from some biologists and zoologists showed that insects mainly take use of the blue and near UV polarized light to realize the orientation [11,12]. In order to mimic the insects' orientation ability, we developed a novel navigation sensor in which we combined Si photodiodes array with blue/violet filters [13]. The usage of filters not only added the sensor's volume but also restricted the miniaturization of the sensor model. Here we presented a novel SOI based photodetector which can eliminate the usage of blue/violet filters. In addition, its device structure and manufacturing process are compatible with subwavelength metal

* Corresponding author at: The Key Laboratory for Micro/Nano Technology and System of Liaoning Province, Dalian University of Technology, Liaoning Dalian 116024, China. Tel.: +86 411 84706108.
*E-mail address:* chujk@dlut.edu.cn (J. Chu).

0038-1101/$ - see front matter © 2010 Elsevier Ltd. All rights reserved.
doi:10.1016/j.sse.2010.09.007

wire-grid polarizers, thus, we can obtain a miniaturized high-performance polarization sensor.

An SOI wafer is consisted of three parts: SOI thin film, BOX and handle wafer. In this paper, a vertical PN junction photodiodes with a SOI layer in thickness of 2.8 μm was designed to achieve high spectral response at shorter wavelength (blue and UV range). Absorption coefficient ($\alpha$) and penetration depth of light in silicon as a function of wavelength are shown in Fig. 1. Penetration depth corresponds to the thickness of Si material which absorbs 63.2% of the incident light. From Fig. 1, we can see that the penetration depth of light with wavelength of 450 nm is only 0.27 μm, which implies that the blue light is absorbed very close to the surface of SOI thin film. Carriers generated in the SOI handle wafer cannot be extracted due to the dielectric BOX. Thus the PN junction photodiode cannot respond to the light which penetrates deeper into the SOI handle wafer.

## 2. Device fabrication

The devices were fabricated on an n-type BESOI wafer provided by Isonics Corp., with a normal resistivity of 3–5 Ω cm (the corresponding doping concentration of phosphorous is about $1 \times 10^{15}$ cm$^{-3}$). The thicknesses of the BOX and the SOI thin film are 1 μm and 2.8 ± 0.5 μm, respectively. The fabrication process was undertaken with the SOI wafer as the starting material. First, the wafer was rinsed by III aqueous (concentrated $H_2SO_4$:$H_2O_2$ = 3:1) and deionized water successively. Next, photolithography was used to define the isolation trench, followed by reactive ion etching (RIE) which etched the SOI thin film through to the BOX layer. After the fabrication of isolation trenches, a $SiO_2$ thin film was grown by using dry oxygen oxidation method at 1000 °C. Successive lithography was used to define the $p^+$ doping area and $n^+$ doping area. With the photoresist as the mask of ion implantation and the $SiO_2$ thin film as the blocking layer, the $p^+$ active area was formed by implanting $BF_2$ ion at an energy of 100 keV and a dose of $1 \times 10^{13}$ cm$^{-2}$. The $n^+$ doping area was formed by using phosphorus ion implantation at an energy of 80 keV and a dose of $5 \times 10^{15}$ cm$^{-2}$. Then, furnace annealing and rapid thermal annealing (RTP) were performed to eliminate the implantation damage and activate the impurity. In order to avoid the spike effect caused by aluminum (Al) metallization and improve the ohmic contact, we initially sputtered a thin layer of titanium (Ti) with the thickness of 0.1 μm, followed by sputtering a thicker layer of Al with the thickness of 0.9 μm. Finally, after the electrode pattern etching, metallization was performed at 430 °C for 30 min under the atmosphere of $N_2$ and $H_2$ mixed gas. The cross-section schematic view of the photodetector is shown as Fig. 2. The active area of the sample photodiode is 1.3 mm × 1.3 mm and the widths of metal contact electrodes in both $p^+$ and $n^+$ doping areas are 50 μm. The width of the surrounding isolation trench is 5 μm.

## 3. Results and discussion

The formation of the shallow PN junction is vital to the photodetector. We simulated the doping condition of the $BF_2$ ion implantation by using Silvaco Athena software [14]. The net doping concentration of boron as a function of depth at active area is shown in Fig. 3. The dotted line marked the interface between the blocking layer of $SiO_2$ and SOI film. The extracted PN junction depth and thickness of surface $SiO_2$ are 262 nm and 70.17 nm, respectively. It can be seen from Fig. 3 that the peak doping concentration of the boron impurity is just located at the interface of the $SiO_2$ and Si. It avoids the formation of reverse drift field which is disadvantageous for the collection of the

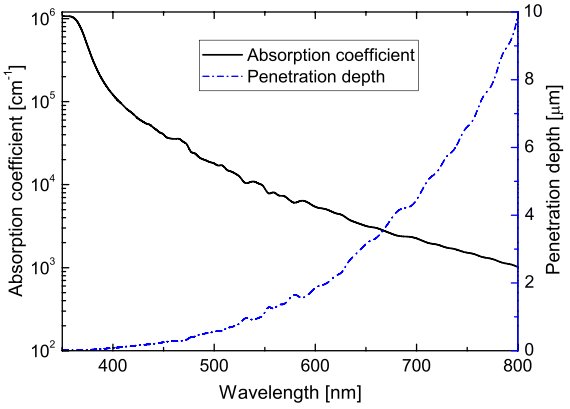


**Fig. 1.** Absorption coefficient and penetration depth of light in Si as a function of wavelength.

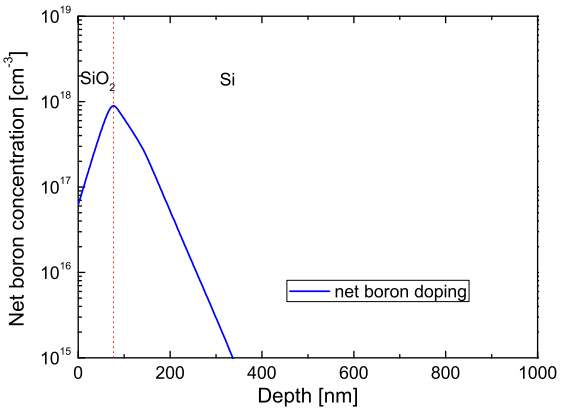


**Fig. 3.** Simulation of the doping condition of the PN junction.

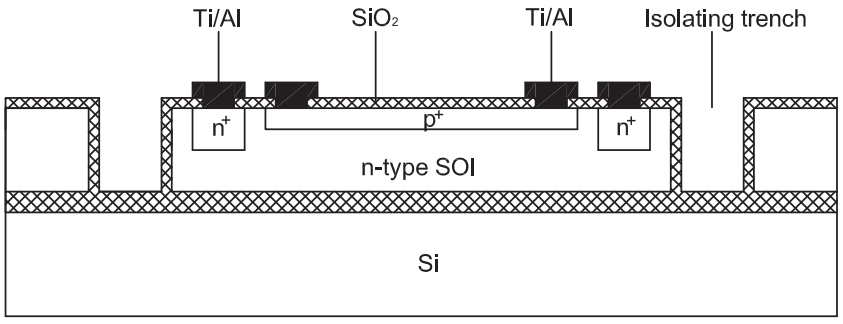


**Fig. 2.** Schematic views of a blue-sensitive Si photodetector in SOI.

photogenerated carriers. Furthermore, the peak concentration of the boron is about $10^{18}\,cm^{-3}$ which is in favor of eliminating the heavy doping effect.

Spectral QE measurements were performed using a tungsten–halogen lamp, grating monochromator (SSM301, Zolix), picoammeter (6485, Keithley), and a reference Si photodetector (S1087-01, Hamamatsu) with known spectral responsivity for photocurrent normalization. The active area of the sample SOI photodetector is 1.3 mm × 1.3 mm which is the same with two types of Hamamatsu photodiodes (S1087 and S1087-01). Compared with the S1087-01 photodiode, the S1087 photodiode had nothing more but a blue filter window. The measurement results of the spectral response are shown in Fig. 4. It shows that the S1087-01 photodiode has high QE over the wide spectral range while the sensitive range of S1087 photodiode is from 360 nm to 720 nm with the peak QE of 73.1% at 540 nm wavelength. However, our sample photodetector achieves the peak external QE of 69.6% at around 480 nm wavelength. Compared with the S1087 photodiode, our device without any filters showed a little blue-shift in spectral response. It should be attributed to the unique characteristic of SOI wafer. Since the absorption coefficient of the shorter wavelength light is very high, the thickness of the thin SOI film is sufficient to absorb most of the photons in the blue and UV region. The thickness of thin SOI film we selected is about 2.8 μm, which is much greater than the penetration depth of blue light. It can make the SOI film absorb shorter wavelength light sufficiently while not increasing the absorption of longer wavelength light too much, which agrees well with the experimental results.

The spectral response of a photodetector is highly dependent on the transmission of light into the semiconductor. One effective solution is to use of a single top layer as an antireflection coating. In our device, we chose the surface $SiO_2$ at the active area to serve as the antireflection coating, which is fabricated by dry oxidation process at 1000 °C. According to the $\lambda/4$ theory (where $\lambda$ denotes the wavelength), we calculated the reflectivity as a function of $SiO_2$ thickness, as shown in Fig. 5a. Since we also take use of the thin $SiO_2$ layer as the blocking layer to improve the ion implantation doping, through which the implanted impurity ion had to penetrate into the SOI film, so we select the $SiO_2$ layer of 70 nm thickness in order to obtain shallow boron doping and reduce the implantation damage at the same time. The reflectivity of 70 nm $SiO_2$ as a function of wavelength is shown in Fig. 5b, from which we can see that, the surface reflectivity has been reduced greatly in the shorter wavelength range.

Due to the difficulty of obtaining SOI wafers in small quantities, the availability of substrate material dictated the thickness

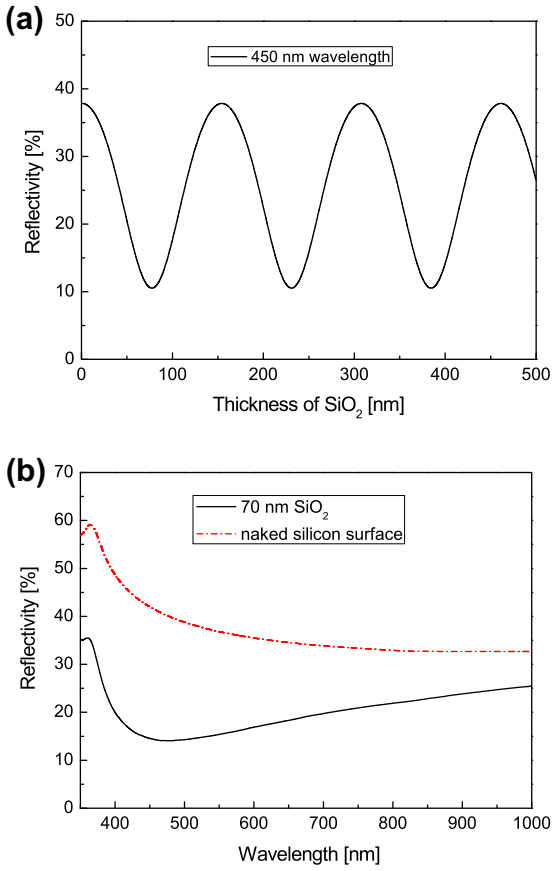


**Fig. 5.** (a) Simulation of surface reflectivity as a function of $SiO_2$ thickness with 450 nm wavelength and (b) simulation of surface reflectivity as a function of wavelength with 70 nm $SiO_2$ thickness.

tolerance of the SOI film. The effect of thickness tolerance of ±0.5 μm on spectral response has been estimated as shown in Fig. 6. The external QE ($\eta$) of the photodetector is calculated as follow:

$$\eta = (1 - R) \cdot [1 - \exp(-\alpha x)] \quad (1)$$

where $R$ denotes the reflectivity at the active area surface; $x$ notes the thickness of the device layer. It can be seen from Fig. 6 that the thickness tolerance has no effect on the spectral response of shorter wavelength. However, the QE of longer wavelength increases gently as the thickness of SOI film increases.

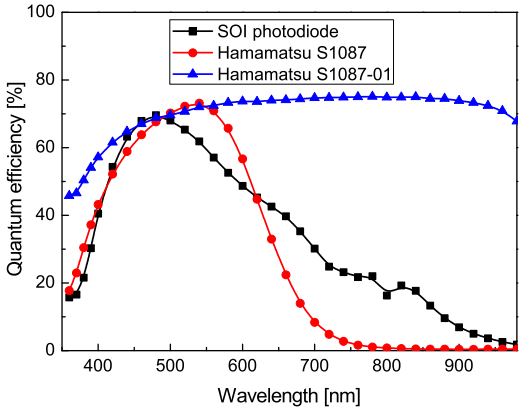


**Fig. 4.** Measurement of quantum efficiency of a sample SOI photodetector and Hamamatsu photodiodes (S1087 and S1087–01).

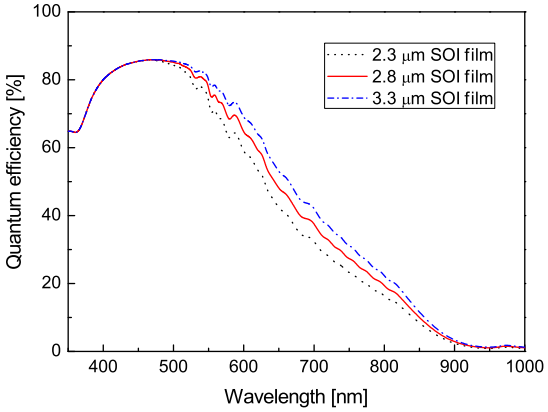


**Fig. 6.** Simulation of quantum efficiency of the photodetector with different SOI film thickness.

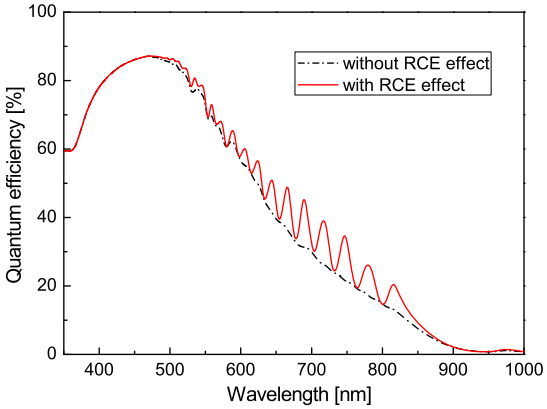


**Fig. 7.** Simulation of quantum efficiency of the SOI photodiode with RCE effect.

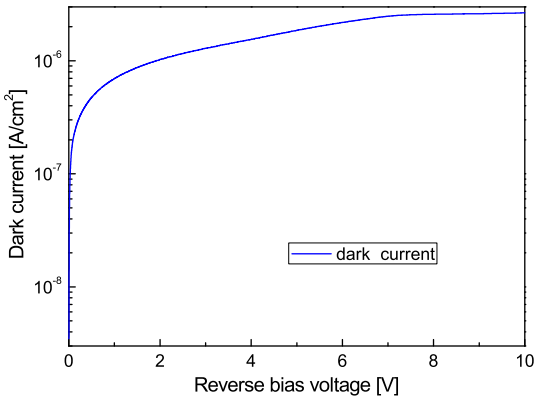


**Fig. 9.** Dark current vs reverse bias voltage of sample SOI photodetector.

In Fig. 4, an obscure oscillation of the spectral response of the sample photodiode can be observed at longer wavelength range which maybe resulted from the resonant cavity enhancement (RCE) effect. When the normal incident light reaches the BOX surface, it will be partially reflected back. So the surface $SiO_2$/SOI film/BOX constitutes a resonant cavity. If we define the RCE factor as $f_{RCE}$, then it can be calculated by [15]:

$$f_{\mathrm{RCE}} = \frac{1 + R_2 e^{-\alpha d}}{1 - 2\sqrt{R_1 R_2}\cdot e^{-\alpha d}\cos\left(\frac{4\pi n d}{\lambda} + \psi_1 + \psi_2\right) + R_1 R_2 e^{-2\alpha d}} \tag{2}$$

where $R_1$ and $R_2$ denotes the reflectivity at the top and bottom surface of the SOI film; $d$ denotes the thickness of the SOI film; $\lambda$ denotes the wavelength of the incident light. If the monochromatic light incidents on the active area normally, $\psi_1 = \psi_2 = 0$. Thus, the external QE can be written:

$$\eta = (1 - R)\cdot[1 - \exp(-\alpha x)]\cdot f_{\mathrm{RCE}} \tag{3}$$

We calculated the QE when taking the RCE effect into consideration. The results are shown in Fig. 7. It can be seen from Fig. 7 that the RCE effect is negligible when $\lambda$ is less than 500 nm, which indicates that the shorter wavelength light has been absorbed completely in the thin SOI film. However, when $\lambda$ is larger than 500 nm, there is a periodical RCE effect on spectral response which agrees well with the measurement results.

To demonstrate the feasibility of our photodetector in measurement of polarized light, we combined the sample photodetectors with polarizing film, then placing them on a rotating platform. The incident light coming from an optical integration sphere was polarized by another piece of polarizing film. The measurement result is shown in Fig. 8, which indicates that our photodetectors have good spectral response to the change of the polarization direction of the polarized light. So our photodetector is feasible to integrate with subwavelength metal wire-grid polarizers functionally.

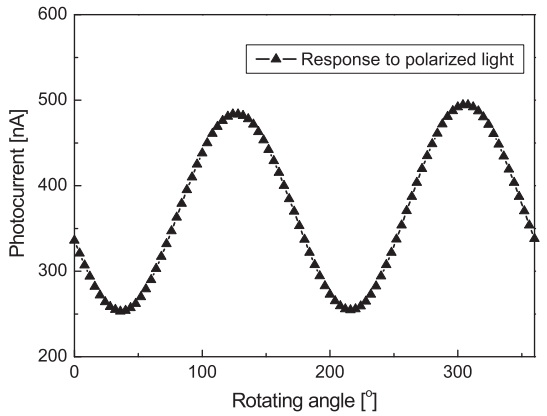


**Fig. 8.** Photocurrent of the sample SOI photodiode as function of rotating angle of platform.

The dark current of the sample photodiode was characterized with Semiconductor Parameter Analyzer (4155B, Agilent). The measurement result is shown in Fig. 9. At the bias voltage of −10 mV, the dark current value is 40.6 nA/cm$^2$, which is much larger than that of Hamamatsu photodiodes (whose dark current level is about 1 nA/cm$^2$). The dark current of PN junction photodiode mainly contains three portions: generation current, diffused current and surface leakage current. At room temperature, the reverse generation current in the space charge region (SCR) is dominant. It can be seen from Fig. 9 that the current increases sharply at the beginning and then increases slowly as the reverse bias voltage increases. This may be explained that: At first, the SCR increase as the reverse bias voltage increases which results in the increase of the dark current abruptly. With the increase of reverse bias voltage, the SOI layer becomes fully depleted, thus the surface leakage current becomes dominant. As the dark current is very sensitive to the surface state density and the fabrication process, we need to reduce the dark current further by an optimized processing in order to achieve a lower defect density in the SOI film and at the $SiO_2$/Si interface.

## 4. Conclusion

In this paper, we presented a novel blue-sensitive photodiode based on SOI wafer. The thin SOI film effectively suppresses the spectral response in longer wavelength of visible light and NIR. So it can eliminate the usage of blue/violet filters in many applications. The external QE of 69.6% is achieved at wavelength of 480 nm. A fully electrical isolation is realized by RIE process. An antireflection coating of single layer of $SiO_2$ was optimized for shorter wavelength. The device structure and manufacturing process are so facile that the photodetector can be monolithically integrated with other micro/nanodevices, such as the subwavelength metal wire-grid polarizers.

## Acknowledgement

The authors would like to thank Microelectronics Process Labs at Peking University for useful discussion and technical service. The work was supported by the State Key Development Program for Basic Research of China (No. 2006CB300407 and No. 2011CB302105), the Fundamental Research Funds for the Central

Universities (No. DUT10ZD104) and the National Science Foundation of China (No. 50775017).

## References

[1] Colinge JP. IEEE Trans Electron Dev 1986;33:203–5.
[2] Ghioni M, Zappa F, Kesan VP, Wamock J. IEEE Trans Electron Dev 1996;33:1054–60.
[3] Li R, Schaub JD, Csutak SM, Campbell JC. IEEE Photon Technol Lett 2000;12:1046–8.
[4] Schaud JD, Li R, Csutak SM, Campbell JC. J Lightwave Technol 2001;19:272–8.
[5] Usami A, Kaneko Y, Fujii Y, Ichimura M. IEEE Trans Electron Dev 1995;42:239–43.
[6] Zimmermann H, Muller B, Hammer A, Herzog K, Seegebrecht P. IEEE Trans Electron Dev 2002;49:334–6.
[7] Zimmermann H, Muller B. IEEE Trans Nucl Sci 2002;49:2032–6.
[8] Afzalian A, Flandre D. IEEE Trans Electron Dev 2005;52:1116–22.
[9] Djuric ZG, Dankovic T, Jaksic ZS, Randjelovic D. Proc. SPIE 1999;3680:601–10.
[10] Afzalian A, Flandre D. Solid-State Electron 2007;51:337–42.
[11] Horváth G, Varjú D. Polarized light in animal vision – polarization patterns in nature. Berlin Heidelberg: Springer-Verlag; 2004.
[12] Stalleicken J, Labhart T, Mouritsen H. J Comp Physiol A 2006;192:321–31.
[13] Chu J, Zhao K, Zhang Q, Wang T. Sens Actuators A: Phys 2008;148:75–82.
[14] ATHENA 2-D process simulator. Santa Clara (CA): SILVACO International; 2005.
[15] Unlu MS, Strite S. J Appl Phys 1995;78:607–39.